Youla Parameterization Based Control Performance Degradation Online Recovery of Single Inverter Control Systems in Microgrids: a PnP Approach

Y. Liu* C. Hu** H. Lu** S.X. Ding* L. Li*** X. Peng**** Y. Wang**

Institute for Automatic Control and Complex Systems, University of Duisburg-Essen, Bismarkstr. 81, BB, 47057, Duisburg, Germany. (e-mail: yannian.liu@uni-due.de).
**College of Electrical and Control Engineering, North China University of Technology, 100144, Beijing, China (e-mail: changbinlove@163.com)*
***School of Automation and Electrical Engineering, University of Science and Technology Beijing, China (e-mail: linlin.li@ustb.edu.cn*
****Key Laboratory of Advanced Control and Optimization for Chemical Processes, East China University of Science and Technology, 200237, Shanghai, China. (xinpeng@ecust.edu.cn)*

Abstract: In an inverter control system of smart microgrids, the control performance degradation due to load fluctuations, unbalanced loads and other factors, is one of the considerable factors affecting the output power quality. In this paper, a plug-and-play (PnP) technology based on Youla parameterization is proposed to achieve system performance recovery without modifying the existing controller. By 'plugging-in' a residual generator and a compensator, a dynamic feed-back of residual signals is embedded into the original inverter control system. In order to realize PnP, an online parameter estimation scheme of the compensator is developed. Finally, an inverter control system is applied to show the effectiveness of the proposed approach.

Keywords: Youla parameterization, performance degradation online recovery, power quality, microgrids

1. INTRODUCTION

Nowadays, micro-grids are attracting more and more attention in research and application with the increasing emphasis on the use of renewable energy in the world and the rapid development of power electronics technology. However, compared with traditional large power grids, the power quality problem of microgrids is more prominent. Firstly, microgrids mainly use clean and environmentally friendly renewable energy sources such as wind and solar energy. Due to environmental impacts, such kind of energy has intermittent and volatility. Secondly, due to the lack of traditional rotating equipment, microgrids have the characteristics of small inertia, weak anti-interference ability, and easy to generate voltage fluctuations. Therefore, the issue of power quality has always been a research hotspot for scholars. Common power quality problems of microgrids mainly include voltage fluctuations, flashing and dips, three-phase unbalances and harmonics.

In general, methodologies to solve power quality problems in microgrids can be broadly divided into passive and ac-

tive governance. The passive governance methods mainly rely on adding a special power management device into the power grids. The most common types of these are reactive power compensation devices, including Static Var Compensator (SVC), Static Synchronous Compensator (STATCOM), Static Var Generator (SVG), etc. (Dixon et al., 2005). Its working principle is to ensure the balance of supply and demand for microgrids by adjusting the reactive power. Furthermore, in order to solve the harmonic problem, a Passive Filter (Peng et al., 1990) is developed. The Unified Power Quality Controller (UPQC) has been proposed, (Ye et al., 2018)-(Kota and Vinnakoti, 2018) to achieve the simultaneous management of multiple power quality problems.

The active governance is based on the element itself, using the same characteristics of inverters in microgrids and some power quality devices, to actively improve the power quality. This not only saves a lot of economic costs but also increases the utilization of inverters in microgrids. In the literature, a great number of methods have been reported on improving voltage imbalances. There are methods such as feeding forward the grid frequency and voltage amplitude to mitigate the impact of grid fluctuation on power flow control (Deng et al., 2016), and an extended droop control strategy to achieve dynamic current sharing

automatically during sudden load changes and resource changes (Xu et al., 2016). In the aspect of the harmonic issues, (Quan et al., 2017) applies linear quadratic control through load current decoupling to achieve the purpose of reducing harmonic content. Further, (Zhong, 2012) improves voltage distortion by achieving harmonic power distribution via the harmonic droop control.

Inspired and motivated by the above observation, a novel strategy of dealing with power quality problems is introduced in this paper. With the purpose of actively solving output power quality problems, such as voltage dips, unbalances and harmonics, and taking full advantage of existing hardware equipment, the Youla parameterization based PnP architecture (Luo, 2017)(Ding et al., 2009)is applied. Via 'plugging-in' a residual generator and a compensator into the original inverter control system, the tracing performance can be greatly recovered online, thereby eliminating output power quality issues caused by external disturbances.

This paper is organized as follows. Section 2 addresses preliminaries and problem formulation. Next, the design procedures for the residual generator, the compensator and the solution of the online optimisation problem are proposed in Section 3. Then three illustrative examples are demonstrated in Section 4 to reveal the effectiveness of the proposed design scheme. At last, Section 5 consists of conclusions of this study based on obtained results.

Notation: The notations in this paper are summarized: $\mathcal{RH}_\infty$ defines the set of all proper and real-rational stable transfer matrices. $\mathbf{G}(z)$ is the discrete-time transfer function matrix. $\mathbf{W}_e$ and $\mathbf{W}_u$ stand for weighting matrices. T_s is the sampling time and k is the k-th discrete-time sample.

2. PRELIMINARIES AND PROBLEM FORMULATION

2.1 Youla parameterization and PnP architecture

Consider a plant $\mathbf{G}(z)$

$$\mathbf{G}(z) = \begin{bmatrix} \mathbf{A} & \mathbf{B} \\ \mathbf{C} & \mathbf{D} \end{bmatrix} \qquad (1)$$

with $\mathbf{G}(z) = \mathbf{N}(z)\mathbf{M}^{-1}(z)$ being the right-coprime and $\mathbf{G}(z) = \hat{\mathbf{M}}^{-1}(z)\hat{\mathbf{N}}(z)$ being the left-coprime factorization. If there exists $\mathbf{X}(z)$, $\mathbf{Y}(z)$, $\hat{\mathbf{X}}(z)$ and $\hat{\mathbf{Y}}(z) \in \mathcal{RH}_\infty$ satisfying the following Bezout identity:

$$\begin{bmatrix} \mathbf{X}(z) & \mathbf{Y}(z) \\ -\hat{\mathbf{N}}(z) & \hat{\mathbf{M}}(z) \end{bmatrix} \begin{bmatrix} \mathbf{M}(z) & -\hat{\mathbf{Y}}(z) \\ \mathbf{N}(z) & \hat{\mathbf{X}}(z) \end{bmatrix} = \begin{bmatrix} \mathbf{I} & 0 \\ 0 & \mathbf{I} \end{bmatrix}, \qquad (2)$$

then through Youla parameterization (Zhou et al., 1996), all feedback controllers that stabilize the plant can be parameterized by (Ding, 2014)

$$\mathbf{K}(z) = -\left(\hat{\mathbf{Y}}(z) + \mathbf{M}(z)\mathbf{Q}(z)\right)\left(\hat{\mathbf{X}}(z) - \mathbf{N}(z)\mathbf{Q}(z)\right)^{-1} \qquad (3)$$

$$= -\left(\mathbf{X}(z) + \mathbf{Q}(z)\hat{\mathbf{N}}(z)\right)^{-1}\left(\mathbf{Y}(z) - \mathbf{Q}(z)\hat{\mathbf{M}}(z)\right), \qquad (4)$$

where $\mathbf{Q}(z) \in \mathcal{RH}_\infty$ is the Youla parameterization matrix. Based on it, the following Theorem is recalled (Ding, 2014), which is essential in the subsequent study.

Theorem 1. Given a control loop with plant model (1) *and a control signal* $u_0(z)$ *provided by the existing controller* $\mathbf{K}_0(z)$ *which internally stabilizes the control loop, then all*

controllers which internally stabilize the control loop can be parameterized by:

$$u(z) = u_0(z) + \mathbf{Q}(z)r(z) \qquad (5)$$

where $\mathbf{Q}(z)$ is a stable parameterization matrix and $r(z)$ is the residual vector available for FDI purposes.
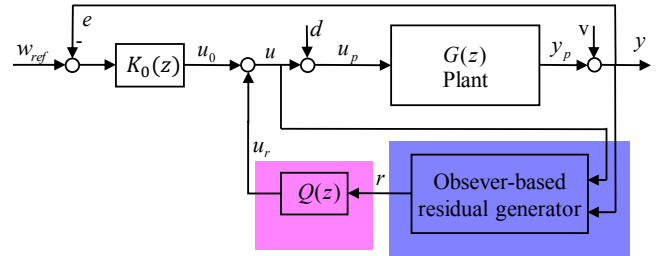
Fig. 1. PnP architecture.

As discussed in (Ding, 2014), $\mathbf{Q}(z) \in \mathcal{RH}_\infty$ only corresponds to the robustness of the closed-loop. Once the system has performance degradation, $\mathbf{Q}(z)r(z)$ can be 'plugged-in' to recover the system performance, as shown in Fig. 1, which is known as the PnP architecture.

2.2 Mechanism analysis of power quality problems in microgrids

In order to solve power quality problems caused by the control performance degradation of micro sources, a mechanism analysis of such power quality issues is requested firstly. To simplify the analysis, three-phase alternating components in microgrids are transformed into direct components in dq coordinate through Clark and Park transform in this paper. According to the different forms of voltage disturbances in the dq rotating coordinate, voltage power quality problems are classified as follows:

- Voltage dips, fluctuations and flickers
  During the operation of microgrids, voltage dips, fluctuations and flickers, caused by, for example, the output power variation due to environmental factors, high-capacity load switching, are transient problems. The control objective is to reduce the deviation of the tracking error and shorten the system response time. Using the constant amplitude method, after the Park transformation matrix, it is clear that when the voltage dips, fluctuates or flickers happen, the load voltage v_o appears as step disturbances in the dq rotating coordinate, in the case of LC loads.

- Voltage unbalances
  The negative sequence component is the root reason for causing the asymmetrical output voltage of inverters, which appears when unbalance loads are accessed into microgrids, such as single-phase load access. According to the symmetrical component method, the three-phase voltage in the abc coordinate can be written in the form of positive and negative zero sequences. Therefore, when the imbalance occurs, the resulting negative sequence component appears as twice rated frequency sinusoid in the dq rotation coordinate.

- Harmonics
  Harmonic disturbances in the voltage are typically caused by accessing non-linear loads in microgrids,

Table 1. Power quality issues and control objectives

Power quality issues	Causes	Representation in the dq axis	Control objectives
voltage dips fluctuations and flickers	dynamic loads, environment	step disturbances	improve response speed
voltage unbalances	unbalanced loads	twice rated frequency	eliminate disturbances effects
harmonics	nonlinear loads	high order sinusoidal	eliminate disturbances effects

including positive, negative and zero sequence components of harmonics. The nth positive and negative sequence components of high frequency harmonics appear as the $(n-1)$th and $(n+1)$th components on the dq axis, respectively.

In summary, the output power quality problems caused by control performance degradation in microgrids and the corresponding control objectives are listed in Table 1.

2.3 Modeling of the plant and problem formulation

From Fig. 2, it is clear that the process is a time-varying nonlinear circuit due to electronic switches. By selecting the average variable of the switch and linearizing it at the operating point, the circuit can be regarded as a linear one between two adjacent switching states. Therefore, consider the LC Filter as the plant and assume that the equivalent gain K_{PWM} of the inverter interface is 1 (Hu et al., 2018) (Hu et al., 2015). According to Kirchhoff's law, the mathematical expression of the plant in the dq coordinate can be obtained as

$$\begin{cases} I_{Ld,k+1} = I_{Ld,k} + T_s(-\dfrac{R_f}{L_f}I_{Ld,k} + \omega I_{Lq,k} + \dfrac{1}{L_f}v_{id,k}) \\[2mm] I_{Lq,k+1} = I_{Lq,k} + T_s(-\dfrac{R_f}{L_f}I_{Lq,k} - \omega I_{Ld,k} + \dfrac{1}{L_f}v_{iq,k}) \\[2mm] v_{od,k+1} = v_{od,k} + T_s(\omega v_{oq,k} + \dfrac{1}{C_f}I_{Ld,k} - \dfrac{1}{C_f}I_{od,k}) \\[2mm] v_{oq,k+1} = v_{oq,k} + T_s(-\omega v_{od,k} + \dfrac{1}{C_f}I_{Lq,k} - \dfrac{1}{C_f}I_{oq,k}) \end{cases}$$

where T_s is the proper sampling time. Now, define $x_{dq,k} = y_{dq,k} = [I_{Ld,k}; I_{Lq,k}; v_{od,k}; v_{oq,k}]$ as state variables and measurement outputs, $u = [v_{id,k}; v_{iq,k}]$ is the plant input and $d_{dq,k} = [I_{od,k}; I_{oq,k}]$ is treated as disturbances. Hence, the state space representation of the plant is formulated as:

$$\begin{cases} x_{dq,k+1} = \mathbf{A}x_{dq,k} + \mathbf{B}u_{dq,k} + \mathbf{E}_d d_{dq,k} \\ y_{dq,k} = \mathbf{C}x_{dq,k} + \mathbf{D}u_{dq,k} \end{cases} \quad (6)$$

where

$$\mathbf{A} = \begin{bmatrix} 1 - T_s\dfrac{R_f}{L_f} & T_s\omega & -T_s\dfrac{1}{L_f} & 0 \\[2mm] -T_s\omega & 1 - T_s\dfrac{R_f}{L_f} & 0 & -T_s\dfrac{1}{L_f} \\[2mm] T_s\dfrac{1}{C_f} & 0 & 1 & T_s\omega \\[2mm] 0 & T_s\dfrac{1}{C_f} & -T_s\omega & 1 \end{bmatrix}, \mathbf{C} = \mathbf{I}_{4\times4},$$

$$\mathbf{B} = \begin{bmatrix} T_s\dfrac{1}{L_f} & 0 \\[2mm] 0 & T_s\dfrac{1}{L_f} \\[2mm] 0 & 0 \\[2mm] 0 & 0 \end{bmatrix}, \mathbf{E}_d = \begin{bmatrix} 0 & 0 \\ 0 & 0 \\ T_s\dfrac{1}{C_f} & 0 \\[2mm] 0 & T_s\dfrac{1}{C_f} \end{bmatrix}, \mathbf{D} = \mathbf{0}_{4\times2}.$$

As discussed in the previous subsections, the external voltage dips, fluctuations and flickers, voltage unbalances and harmonics, which are all reflected in $d_{dq,k}$ of (6), can cause control performance degradation, and this ultimately will affect the output power quality of the inverter control system. With the purpose of eliminating the control performance degradation, the PnP architecture, Fig.1, will be embedded into an existing inverter control system. In this way, the control performance can be recovered without modifying the original control loop. Furthermore, to develop a general form of the compensator $\mathbf{Q}(z)$ facing different applications, one online estimation scheme of $\mathbf{Q}(z)$ needs proposing.

3. DESIGN SCHEMES

3.1 State-space representation of voltage and current double closed-loop decoupling controller

The voltage and current double closed-loop decoupling controller is one of the most frequently used controllers in inverter-based microgrid systems. Many types of research have been studied, for instance, (Hu et al., 2018). Basically it is constructed based on four PI controllers with decoupling loops to solve the coupling problems in the plant of LC filters. The mathematical description in the discrete form can be rewritten as:

$$\begin{cases} I_{Ld}^* = -\omega C_f v_{oq} + K_{pv}T_s(v_{od}^* - v_{od}) + K_{iv}\phi_d \\ I_{Lq}^* = \omega C_f v_{od} + K_{pv}T_s(v_{oq}^* - v_{oq}) + K_{iv}\phi_q \\ v_{id}^* = -\omega L_f I_{Lq} + K_{pc}T_s(I_{Ld}^* - I_{Ld}) + K_{ic}\gamma_d \\ v_{iq}^* = \omega L_f I_{Ld} + K_{pc}T_s(I_{Lq}^* - I_{Lq}) + K_{ic}\gamma_q \end{cases}$$

where K_{pv}, K_{pc} and K_{iv}, K_{ic} are the designed parameters of PI controllers for voltage and current control loop respectively; ϕ_d, ϕ_q, γ_d, γ_q are defined states, which has

$$\phi_{d,k+1} - \phi_{d,k} = v_{od,k}^* - v_{od,k}, \quad \phi_{q,k+1} - \phi_{q,k} = v_{oq,k}^* - v_{oq,k}$$
$$\gamma_{d,k+1} - \gamma_{d,k} = I_{ld,k}^* - I_{ld,k}, \quad \gamma_{q,k+1} - \gamma_{q,k} = I_{lq,k}^* - I_{lq,k}.$$

Then, the discrete state-space representation of the double closed-loop controller can be obtained, by introducing the tracing errors

$$e_{idq} = I_{Ldq}^* - I_{Ldq}, \quad e_{vdq} = v_{odq}^* - v_{odq},$$

then

$$\begin{bmatrix} \gamma_{dq,k+1} \\ \phi_{dq,k+1} \end{bmatrix} = \mathbf{A}_{vcz}\begin{bmatrix} \gamma_{dq,k} \\ \phi_{dq,k} \end{bmatrix} + \mathbf{B}_{vcz}\begin{bmatrix} e_{idq,k} \\ e_{vdq,k} \end{bmatrix} \quad (7)$$

$$\begin{bmatrix} v_{id}^* \\ v_{iq}^* \end{bmatrix} = \mathbf{C}_{vcz}\begin{bmatrix} \gamma_{dq} \\ \phi_{dq} \end{bmatrix} + \mathbf{D}_{vcz1}\begin{bmatrix} e_{idq} \\ e_{vdq} \end{bmatrix} + \mathbf{D}_{vcz2}u_{con} \quad (8)$$

where $\mathbf{A}_{vcz}$, $\mathbf{B}_{vcz}$ $\mathbf{D}_{vcz2}$ are $\mathbf{I}_{4\times4}$, $T_s\mathbf{I}_{4\times4}$, $\mathbf{I}_{2\times2}$ respectively, $\mathbf{C}_{vcz}$, $\mathbf{D}_{vcz1}$, the constant component u_{con} presents as

$$\mathbf{C}_{vcz} = \begin{bmatrix} K_{ic} & 0 & 0 & -L_f\omega K_{iv} \\ 0 & K_{ic} & L_f\omega K_{iv} & 0 \end{bmatrix},$$

$$\mathbf{D}_{vcz1} = \begin{bmatrix} K_{pc} & L_f\omega & L_fC_f\omega^2 & -L_f\omega K_{pv} \\ -L_f\omega & K_{pc} & L_f\omega K_{pv} & L_fC_f\omega^2 \end{bmatrix},$$

$$u_{con} = \begin{bmatrix} -C_f L_f \omega^2 v_{od}^* \\ -C_f L_f \omega^2 v_{oq}^* \end{bmatrix}.$$

In order to obtain the 6-phase PWM (Pulse Width Modulation) wave, the two-phase DC control signal is converted by dq/abc to obtain a 3-phase sine modulation wave, thereby controlling electronic switches.

3.2 Residual generator design

In this paper, the following residual generator is adopted:

$$\begin{cases} z_{dq,k+1} = \mathbf{A} z_{d,q,k} + \mathbf{B} u_{d,q,k} + \mathbf{L}_o r_k \\ \hat{y}_{d,q,k} = \mathbf{C} z_{d,q,k} + \mathbf{D} u_{d,q,k} \\ r_k = y_{d,q,k} - \hat{y}_{d,q,k} \end{cases} \quad (9)$$

where $\mathbf{L}_o$, chosen to ensure the stability of $\mathbf{A} - \mathbf{L}_o \mathbf{C}$, is the gain matrix of the observer and $z_{dq}(k)$ is the state's estimation; $\hat{y}_{dq}$ and $r(k)$ represent the output estimation and residual signal respectively with

$$r_k = [r_{ILd}; r_{ILq}; r_{vod}; r_{voq}], \hat{y}_{d,q}(k) = [\hat{I}_{Ld}; \hat{I}_{Lq}; \hat{v}_{od}; \hat{v}_{oq}].$$

3.3 Design of compensator $\mathbf{Q}(z)$

In (Luo, 2017), the general form of optimizing $\mathbf{Q}(z)$ has been well studied. While in this paper, it is mainly concentrated on the design scheme for the inverter control system. The compensator $\mathbf{Q}(z)$ is designed to reduce the amount of online calculation and fulfill the control objective. Start with the state-space mathematical model, the parameterized $\mathbf{Q}(z)$ in the corresponding discrete state is:

$$\begin{cases} x_{r,k+1} = \mathbf{A}_r x_{r,k} + \mathbf{B}_r r_k \\ u_{r,k} = \mathbf{C}_r x_{r,k} + \mathbf{D}_r r_k, \end{cases} \quad (10)$$

where the states $x_r = [x_{r,ILd}; x_{r,Lq}; x_{r,Vod}; x_{r,Voq}]$ and the output signal $u_r = [u_{r,Vod}; u_{r,Voq}]$, which is fed back and added to the output of original controller. Furthermore, $\mathbf{A}_r$, $\mathbf{B}_r$, $\mathbf{C}_r$, and $\mathbf{D}_r$ are formulated from

$$u_{rd,k} = \frac{\delta_1}{z-T} r_{ILd} + \frac{\delta_2}{z-T} r_{vod} + \delta_5 r_{ILd} + \delta_6 r_{vod}$$

$$u_{rq,k} = \frac{\delta_3}{z-T} r_{ILq} + \frac{\delta_4}{z-T} r_{voq} + \delta_7 r_{ILq} + \delta_8 r_{voq}$$

where $T \in (-1, 1)$, which guarantees $\mathbf{Q}(s) \in \mathcal{RH}_\infty$, and $u_{rd,k}$, $u_{rq,k}$ are designed for the dq-axis decoupling purpose.

3.4 Online optimisation problem formulation and parameters update

In order to online estimate the parameters of $\mathbf{Q}(s)$, one online optimization problem will be formulated in this subsection. To solve previously introduced power quality problems, it is necessary to reduce the tracking error e of the inverter control system in microgrids. However, the closed-loop dynamic stability shown in Fig. 1 needs to be guaranteed firstly, after 'plugging-in' the residual generator and $\mathbf{Q}(s)$. Combined with equations (7),(8) (9) and (10), its state-space representation comes into being

$$\begin{bmatrix} z_{d,q,k+1} \\ x_{c,k+1} \\ x_{r,k+1} \end{bmatrix} = \mathbf{A}_{cl} \begin{bmatrix} z_{d,q,k} \\ x_{c,k} \\ x_{r,k} \end{bmatrix} + \mathbf{B}_{1,cl} \begin{bmatrix} w_{ref,k} \\ r_k \end{bmatrix} + \mathbf{B}_{2,cl} u_{con} \quad (11)$$

$$\begin{bmatrix} e_k \\ u_k \end{bmatrix} = \mathbf{C}_{cl} \begin{bmatrix} z_{d,q,k} \\ x_{c,k} \\ x_{r,k} \end{bmatrix} + \mathbf{D}_{1,cl} \begin{bmatrix} w_{ref,k} \\ r_k \end{bmatrix} + \mathbf{D}_{2,cl} u_{con} \quad (12)$$

where

$$\mathbf{A}_{cl} = \begin{bmatrix} \mathbf{A} - \mathbf{B} \mathbf{D}_{vc1} \mathbf{C} & \mathbf{B} \mathbf{C}_{vc} & \mathbf{B} \mathbf{C}_r \\ -\mathbf{B}_{vc1} \mathbf{C} & \mathbf{A}_{vc} & 0 \\ 0 & 0 & \mathbf{A}_r \end{bmatrix}, \mathbf{B}_{2,cl} = \begin{bmatrix} \mathbf{B} \mathbf{D}_{vc2} \\ 0 \\ 0 \end{bmatrix},$$

$$\mathbf{B}_{1,cl} = \begin{bmatrix} \mathbf{B} \mathbf{D}_{vc1} & \mathbf{B}(\mathbf{D}_r - \mathbf{D}_{vc1}) + \mathbf{L}_o \\ \mathbf{B}_{vc1} & -\mathbf{B}_{vc1} \\ 0 & \mathbf{B}_r \end{bmatrix}, \mathbf{D}_{2,cl} = \begin{bmatrix} 0 \\ \mathbf{D}_{vc2} \end{bmatrix},$$

$$\mathbf{C}_{cl} = \begin{bmatrix} -\mathbf{C} & 0 & 0 \\ -\mathbf{D}_{vc1} \mathbf{C} & \mathbf{C}_{vc} & \mathbf{C}_r \end{bmatrix}, \mathbf{D}_{1,cl} = \begin{bmatrix} \mathbf{I} & -\mathbf{I} \\ \mathbf{D}_{vc1} & \mathbf{D}_r - \mathbf{D}_{vc1} \end{bmatrix}.$$

Then, the stability of the closed-loop (11), (12) is ensured, when $\mathbf{A}_{cl}$ is stable. Therefore, together with taking into account less consuming of control energy u and stable constraints, the online iterative optimization problem is considered:

$$\min J_N^{j,\theta_j} = \frac{1}{2N} \sum_{k=k_j}^{N+k_j-1} \left\{ e_{\theta_j,k}^T \mathbf{W}_e e_{\theta_j,k} + u_{\theta_j,k}^T \mathbf{W}_u u_{\theta_j,k} \right\}$$

$$s.t. \quad \theta_{j,T} \in (-1, 1) \quad (13)$$

$$\begin{bmatrix} \mathbf{A} - \mathbf{B} \mathbf{D}_{vc1} \mathbf{C} & \mathbf{B} \mathbf{C}_{vc} \\ -\mathbf{B}_{vc1} \mathbf{C} & \mathbf{A}_{vc} \end{bmatrix} \text{ is stable}$$

where integers k_j and N are the starting sampling instant of jth iteration and the time window; $\mathbf{W}_e$ and $\mathbf{W}_u$ are positive constant weighting factors; and θ_j is the parameter vector of $\mathbf{Q}(z)$ (10), $\theta_j = [T_j; \delta_i], i = 1, ..., 8$, as designed in (10). To solve the optimisation problem (13), the *Gauss-Newton method* is applied and the parameters update rule is formulated according to the steepest-descent step as

$$\theta_{j+1} = \theta_j - \mathbf{\Phi} \frac{\partial J_N^{j,\theta_j}}{\partial \theta_j} |_{\theta_{j-1}}, \quad (14)$$

where $\mathbf{\Phi} > 0$ is the step size of jth iteration and

$$\frac{\partial J_N^{j,\theta_j}}{\partial \theta_j} = \frac{1}{N} \sum_{k=k_j}^{N+k_{j-1}-1} \left\{ e_{\theta_{j-1},k}^T \mathbf{W}_e e_{\theta_{j-1},k} + u_{\theta_{j-1},k}^T \mathbf{W}_u u_{\theta_{j-1},k} \right\}. \quad (15)$$

Subsequently, with the purpose of iteratively online estimation (Luo, 2017) of $\partial J_N^{j,\theta_j}/\partial \theta_j$, following equations are constructed:

i. Gradient estimation for $\theta_{j,T}$

$$\frac{\partial x_{g,k+1}^{\theta_{j,T}}}{\partial \theta_{j,T,k+1}} = \mathbf{A}_{g,\theta_j} \frac{\partial x_{g,k}^{\theta_{j,T}}}{\partial \theta_{j,T,k}} + \begin{bmatrix} 0 \\ 0 \\ \mathbf{I}_{4 \times 4} \end{bmatrix} x_{r,k}^{\theta_j} \quad (16)$$

$$\begin{bmatrix} \frac{\partial e_{g,k}^{\theta_{j,T}}}{\partial \theta_{j,T,k}} \\ \frac{\partial u_{g,k}^{\theta_{j,T}}}{\partial \theta_{j,T}, k} \end{bmatrix} = \begin{bmatrix} -\mathbf{C} & 0 & 0 \\ -\mathbf{D}_{vc1} \mathbf{C} & \mathbf{C}_{vc} & \mathbf{C}_{r,\theta_{j,k_i}} \end{bmatrix} \frac{\partial x_{g,k}^{\theta_{j,T}}}{\partial \theta_{j,T,k}} \quad (17)$$

where

$$\mathbf{A}_{g,\theta_j} = \begin{bmatrix} \mathbf{A} - \mathbf{B} \mathbf{D}_{vc1} \mathbf{C} \mathbf{B} \mathbf{C}_{vc} & \mathbf{B} \mathbf{C}_r^{\theta_{j,\delta_i}} \\ -\mathbf{B}_{vc1} \mathbf{C} & \mathbf{A}_{vc} & 0 \\ 0 & 0 & \mathbf{A}_r^{\theta_{j,T}} \end{bmatrix}$$

for $i = 1, .., 4$ as presented in equation (10) and $\theta_{j,T,k}$ is the T element of θ_j in the kth iteration.

ii. Gradient estimation for $\delta_i, i = 1, .., 4$

$$\frac{\partial x_{g,k+1}^{\theta_{j,\delta_i}}}{\partial \theta_{j,\delta_i,k+1}} = \mathbf{A}_{go} \frac{\partial x_{g,k}^{\theta_{j,\delta_i}}}{\partial \theta_{j,\delta_i,k}} + \begin{bmatrix} \mathbf{B} \frac{\partial \mathbf{C}_{r,k}^{\theta_{j,\delta_i}}}{\partial \theta_{j,\delta_i,k}} \\ 0 \end{bmatrix} x_{r,k}^{\theta_{j,\delta_i}} \quad (18)$$

Table 2. Parameters settings

Name	L_f	C_f	R_f	K_{pv}	K_{iv}	K_{pc}	K_{ic}	T_s
Value	$2mH$	$150\mu H$	0.01Ω	10	100	10	0	$0.5\mu s$

$$\begin{bmatrix} \dfrac{\partial e_{g,k}^{\theta_j,\delta_i}}{\partial \theta_{j,\delta_i,k}} \\ \dfrac{\partial u_{g,k}^{\theta_j,\delta_i}}{\partial \theta_{j,\delta_i,k}} \end{bmatrix} = \begin{bmatrix} -\mathbf{C} & \mathbf{0} \\ -\mathbf{D}_{vc1}\mathbf{C} & \mathbf{C}_{vc} \end{bmatrix} \dfrac{\partial x_{g,k}^{\theta_j,\delta_i}}{\partial \theta_{j,\delta_i,k}} + \begin{bmatrix} \mathbf{0} \\ \dfrac{\partial \mathbf{C}_{r,k}^{\theta_j,\delta_i}}{\partial \theta_{j,\delta_i,k}} \end{bmatrix} x_{r,k}^{\theta_j,\delta_i} \quad (19)$$

where

$$\mathbf{A}_{go} = \begin{bmatrix} \mathbf{A} - \mathbf{B}\mathbf{D}_{vc1}\mathbf{C} & \mathbf{B}\mathbf{C}_{vc} \\ -\mathbf{B}_{vc1}\mathbf{C} & \mathbf{A}_{vc} \end{bmatrix},$$

with $\theta_{j,\delta_i,k}$ is the $\delta_i, i = 1,...,4$ element of θ_j in the kth iteration.

iii. Gradient estimation for $\delta_i, i = 5,..,8$

$$\dfrac{\partial x_{g,k+1}^{\theta_j,\delta_i}}{\partial \theta_{j,\delta_i,k+1}} = \mathbf{A}_{go} \dfrac{\partial x_{g,k}^{\theta_j,\delta_i}}{\partial \theta_{j,\delta_i,k}} + \begin{bmatrix} \mathbf{B}\dfrac{\partial \mathbf{D}_{r,k}^{\theta_j,\delta_i}}{\partial \theta_{j,\delta_i,k}} \\ \mathbf{0} \end{bmatrix} r_k \quad (20)$$

$$\begin{bmatrix} \dfrac{\partial e_{g,k}^{\theta_j,\delta_i}}{\partial \theta_{j,\delta_i,k}} \\ \dfrac{\partial u_{g,k}^{\theta_j,\delta_i}}{\partial \theta_{j,\delta_i,k}} \end{bmatrix} = \begin{bmatrix} -\mathbf{C} & \mathbf{0} \\ -\mathbf{D}_{vc1}\mathbf{C} & \mathbf{C}_{vc} \end{bmatrix} \dfrac{\partial x_{g,k}^{\theta_j,\delta_i}}{\partial \theta_{j,\delta_i,k}} + \begin{bmatrix} \mathbf{0} \\ \dfrac{\partial \mathbf{D}_{r,k}^{\theta_j,\delta_i}}{\partial \theta_{j,\delta_i,k}} \end{bmatrix} r_k, \quad (21)$$

where $\theta_{j,\delta_i,k}$ is the $\delta_i, i = 5,...,8$ element of θ_j in the kth iteration. At last, the proposed online iterative configuration can be summarized in the Algorithm 1.

Algorithm 1 Control performance degradation recovery

---

1. Design the residual generator and compensator $\mathbf{Q}(z)$ as (9) and (10).
2. Construct the gradient estimator according to (16)-(21) and set related initial state be zero.
3. Initialize $j = 0$, $\theta_0 = 0$, the stop criteria $\epsilon > 0$, time window $N > 0$, $\mathbf{W}_e, \mathbf{W}_u > 0$ and define a proper update step size $\mathbf{\Phi}$.
4. Collect e_k, u_k r_k and gradients from starting time k_0 to $k_0 + N - 1$.
5. Calculate J_N^{j,θ_j} and $\frac{\partial J_N^{j,\theta_j}}{\partial \theta_j}$ through (13) and (15).
6. Update θ_j accolading 14.
7. If $\theta_{j,T} \notin (-1,1)$, set $\theta_{j,T} = \theta_{j-1,T}$.
8. Reconstruct the compensator $\mathbf{Q}_j(z)$ based on (10).
9. Set $j = j + 1$ and $k_0 = N + k_0$.
10. Go back to step 5 until all the parameters in θ_j converged or the stop condition $J_N^{j,\theta_j} - J_N^{j-1,\theta_{j-1}} < \epsilon$.

3.5 Overall control strategy

From the previous study, the PnP approach of performance degradation recovery strategy of inverter control systems in microgrids is shown as Fig. 2.

4. SIMULATION RESULTS

In order to verify the effectiveness of the proposed performance degradation recovery method for inverter systems, one simulation example is implemented in the Matlab/Simulink, with the parameter settings as shown in Table 2. Firstly, use cut-in/cut-out loads to simulate voltage dips, fluctuations or flickers. This example is done with the
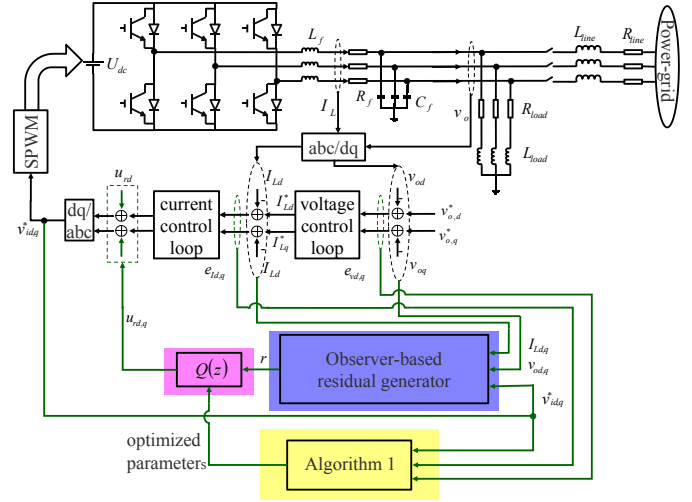
Fig. 2. Schematic diagram of power quality control of voltage source inverters in microgrids.

assumption of sudden active load power increasing from $6kW$ to $20kW$ at the 1 second, then abrupt decreasing back to 6 kW at the 2nd second. After 1 second, the load power increases back to $20kW$ again. Take this process as a period to simulate frequent active load switchings. Fig. 3 shows the simulation result. In the 2nd second,
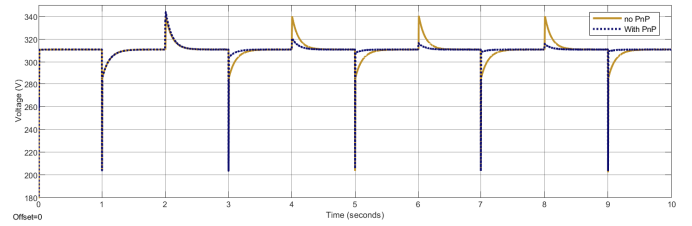
Fig. 3. d-axis component voltage.

the designed performance degradation recovery unite is 'plugged-in'. Compared with the output voltage of the original control loop (dashed line), after $3 - 4$ iterations, the output voltage performance degradation is greatly improved. In this way, microgrid inverter systems can be more reliable to supply power under the condition of voltage dips, fluctuations or flickers. The purpose of improving the output power quality of inverter systems in microgrids is achieved.

Next, an unbalanced load is constructed to verify the performance improvement in voltage imbalance. The three-phase resistive load (10Ω) adopts the star type ungrounded mode. At 0.5th second, the load of phase 'c' is open. Fig. 4 gives the simulation results after 'plug-in' the performance degradation recovery unit. It is clear that the three-phase output voltage imbalance is amazingly improved only after a few iterations.

At last, a non-linear load is connected to the inverter system, in order to create a harmonic environment. As in the first two examples, the proposed performance degradation recovery strategy is 'plugged in' at the selected 2nd second. The harmonic components of the phase 'a' are shown in Fig. 5. With the embedded compensation loop, the high frequency-harmonics are significantly suppressed, from about 5.32% to 0.64%.

(a) *d*-axis
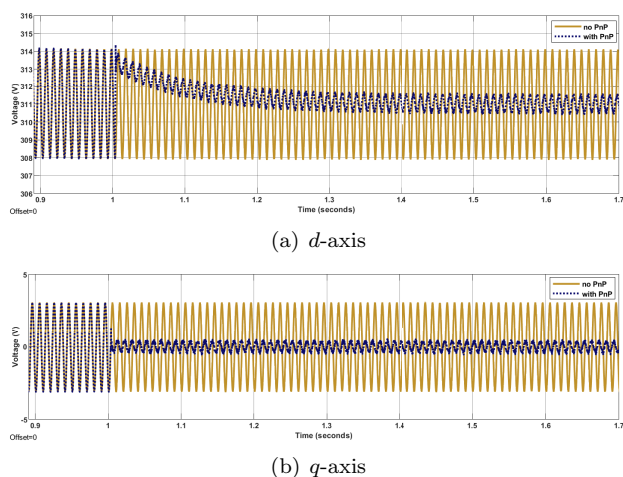
(b) *q*-axis

Fig. 4. *dq*-axis component voltage.

(a) no PnP

(b) with PnP
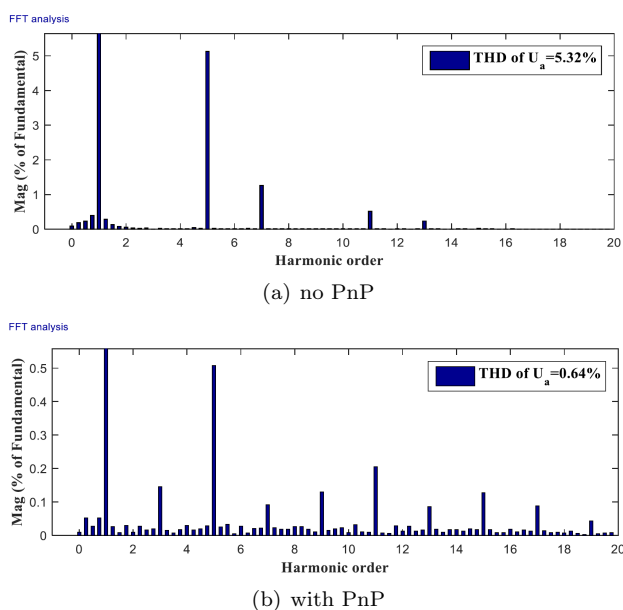
Fig. 5. Harmonic components of *dq*-axis in a-phase voltage.

5. CONCLUSION

This paper proposes a strategy to improve the power quality of inverter systems in microgrids, by recovering control performance. At the same time, the effectiveness is proved by three experimental simulations. This proves that the proposed strategy could well solve the output power quality problems caused by such as external voltage dips, fluctuations or flickers, imbalance and harmonics in inverter systems. Nevertheless, it should be pointed out that more in-depth and detailed work still needs to be done, for example, verification in real systems, different forms of $Q(z)$ design, research in multi-inverter parallel systems, and so on.

REFERENCES

Deng, Y., Tao, Y.and Chen, G., Li, G., and He, X. (2016). Enhanced power flow control for grid-connected droop-controlled inverters with improved stability. *IEEE Transactions on Industrial Electronics*, 64(7), 5919–5929.

Ding, S.X. (2014). *Model-based fault diagnosis techniques: design schemes, algorithms, and tools.* Springer Science & Business Media.

Ding, S., Yang, G., Zhang, P.and Ding, E.L., Jeinsch, T., Weinhold, N., and Schultalbers, M. (2009). Feedback control structures, embedded residual signals, and feedback control schemes with an integrated residual access. *IEEE Transactions on Control Systems Technology*, 18(2), 352–367.

Dixon, J., Moran, L., Rodriguez, J., and Domke, R. (2005). Reactive power compensation technologies: State-of-the-art review. *Proceedings of the IEEE*, 93(12), 2144–2164.

Hu, C., Luo, S., Li, Z., Wang, X., and Sun, L. (2015). Energy coordinative optimization of wind-storage-load microgrids based on short-term prediction. *Energies*, 8(2), 1505–1528.

Hu, C., Wang, Y., Luo, S., and Zhang, F. (2018). State-space model of an inverter-based micro-grid. In *2018 3rd International Conference on Intelligent Green Building and Smart Grid (IGBSG)*, 1–7. IEEE.

Kota, V. and Vinnakoti, S. (2018). Performance evaluation of upqc under nonlinear unbalanced load conditions using synchronous reference frame based control. *Journal of The Institution of Engineers (India): Series B*, 99(1), 37–48.

Luo, H. (2017). *Plug-and-Play Monitoring and Performance Optimization for Industrial Automation Processes.* Springer.

Peng, F., Akagi, H., and Nabae, A. (1990). A new approach to harmonic compensation in power systems-a combined system of shunt passive and series active filters. *IEEE Transactions on industry applications*, 26(6), 983–990.

Quan, X., Dou, X., Hu, M., and Huang, A.Q. (2017). Load current decoupling based lq control for three-phase inverter. *IEEE Transactions on Power Electronics*, 33(6), 5476–5491.

Xu, Q.and Hu, X., Wang, P.and Xiao, J., Tu, P., and Wen, C.and Lee, M. (2016). A decentralized dynamic power sharing strategy for hybrid energy storage system in autonomous dc microgrid. *IEEE transactions on industrial electronics*, 64(7), 5930–5941.

Ye, J., Gooi, H., and Wu, F. (2018). Optimal design and control implementation of upqc based on variable phase angle control method. *IEEE Transactions on Industrial Informatics*, 14(7), 3109–3123.

Zhong, Q. (2012). Harmonic droop controller to reduce the voltage harmonics of inverters. *IEEE Transactions on Industrial Electronics*, 60(3), 936–945.

Zhou, K., Doyle, J.C., Glover, K., et al. (1996). *Robust and optimal control*, volume 40. Prentice hall New Jersey.